Modeling of an Insect Proprioceptor System based on Different Neuron Response Times

Daniel Rodrigues de Lima[1], Michel Bessani[1], Philip Newland[2] and Carlos Dias Maciel[1]
[1]*Department of Electrical and Computational Engineering, University of São Paulo, São Carlos, São Paulo, Brazil*
[2]*Centre for Biological Science, University of Southampton, Highfield Campus, S017 1BJ Southampton, U.K.*

Keywords: Neuronal Spike Signals, Neuronal Response, Desert Locust, FeCO, Transfer Entropy, Inter-Spike Interval, Survival Analysis.

Abstract: This paper analyzes neuronal spiking signals from the Desert Locust Femorotibial Chordotonal Organ (FeCO). The data comes from records of the insect neuronal response due to external stimulation. We measured the Inter-Spike Interval (ISI) and calculated Transfer Entropy for investigate different FeCO responses. ISI is a technique that measures the time between two spikes; and transfer entropy is a theoretical information measure used to find dependencies and causal relationships. We also use survival functions to assemble FeCO models. Furthermore, this work uses and compares results of two approaches, one with transfer entropy and other with ISI measures. The results indicate evidence to support the existence of more than one type of FeCO neuron.

1 INTRODUCTION

The biologically inspired engineering studies biological structures intending to find solutions for engineering problems (Zhang et al., 2015). Examples include the Particle Swarm Optimization Algorithm (Santos and Maciel, 2014), the control of exoskeletons using principles found in biomechanics (Jimnez-Fabin and Verlinden, 2012) and neuronal circuits (Endo et al., 2015). Recent works analyzed neural signals (Jegadeesan et al., 2015) trying to identify patterns and connections inside the nervous system (Subramaniam et al., 2015). They analyzed signals from neural experiments which are records from the neuronal responses due to some specific stimulus or situations (Birmingham et al., 2014).

This paper presents the analysis of signals collected on experiments with desert locust neurons. The experiments were made by stimulating the insect lag with a forceps that was shaken by a Gaussian White Noise (GWN). Figure 1 shows the signal analysis schematic and presents a sample of the recorded signals. The data analyzed come from a large and multivariate neurobiological data set obtained from a neural insect network (Newland and Kondoh, 1997). This network produces and controls the movements of the desert locust hind leg (Angarita-Jaimes et al., 2012). Specifically, the data analyzed here were collected on the Femorotibial Chordotonal Organ (FeCO). FeCO is a proprioceptor that detects movements from the tibia relative to the femur of a desert locust hind leg (Burrows et al., 1988), and its behavior is equivalent to others found in more complex structures (Vidal-Gadea et al., 2010).

Previous studies investigated neuronal structure models in the FeCO data (Maciel et al., 2012). They also investigated characteristics of the signal transmission channel (Endo et al., 2015). While doing these experiments, transfer entropy measurements (Schreiber, 2000) suggested the existence of different kinds of FeCO. Transfer entropy is an information-theoretic measurement, which allows to detect non-linearity (Nichols et al., 2005), establish causal relationships (Barnett et al., 2009), and also find interaction delays between signals (Pampu et al., 2013). Some curves obtained from these measurements showed different FeCO responses and pointed the possible existence of different groups of neurons. Those curves motivated this investigation about how many kinds of FeCO neurons exist.

In order to investigate different FeCO responses we combined two analyzes: transfer entropy and the Inter-Spike Interval (ISI) (Schwalger et al., 2015). Classically, ISI measures the amount of time spent between spikes, trying to find a probability distribution for them (Chen et al., 2009). However, this study uses ISI measurements to determine parameters to classify the FeCO in different groups of neurons. The pa-

Lima, D., Bessani, M., Newland, P. and Maciel, C.
Modeling of an Insect Proprioceptor System based on Different Neuron Response Times.
DOI: 10.5220/0005706202190226
In *Proceedings of the 9th International Joint Conference on Biomedical Engineering Systems and Technologies (BIOSTEC 2016) - Volume 4: BIOSIGNALS*, pages 219-226
ISBN: 978-989-758-170-0

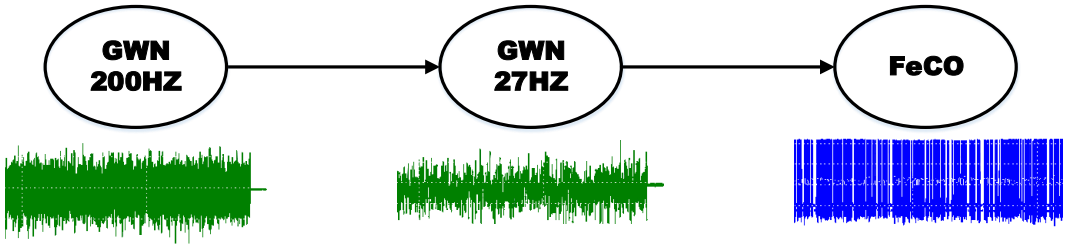

Figure 1: Schematic of the signal analysis presenting the collected signals (bottom) and their interaction (top). In the experiment, a Gaussian Withe Noise (GWN) with a bandwidth of 200Hz passed trough a low-pass filter with cutoff frequency manually adjusted to 27Hz or 58Hz. The filtered signal shook a forceps that moved the locust leg stimulating its nervous system. The FeCO signal is the neuronal response to the excitation, and it is also a spiking signal. This diagram is the primary assumption, which considers only one kind of FeCO.

rameters found are used in a statistical representation, which uses survival functions (Lawless, 2011) to assemble FeCO models.

Survival Analysis aims to explore the behavior of sets of individuals according to the time interval necessary for an event to happen (Collett, 2003). Examples include a system failure (Achcar and Moala, 2015) or a patient longevity (MacKenzie et al., 2014). The survival technique also analyzes data from remission time (Cabrero et al., 2015), which is the time spent between two occurrences of an event (Bewick et al., 2004). ISI is the time spent between two spikes (two occurrences), and it is possible to use survival functions to create FeCO models.

The study goal is to investigate whether the FeCO response rates would change under the same stimulation. For that, we analyzed FeCO signals recorded during two different experiments: one applying a GWN stimulation limited to 27Hz; and another limited to 58Hz. To perform the analysis, we used ISI technique and statistical treatments as a criterion to divide and classify the signals into different groups.

We also used transfer entropy to reinforce our assumption about the existence of different kinds of FeCO and investigate the differences between the groups found. Finding different types of FeCO, the diagram in Figure 1 will need to be changed. This study will be useful then to check if the diagram from Figure 1 is sufficient to represent the FeCO neuronal structure or if a more complex model is required.

Furthermore, using the two analyzes, ISI and transfer entropy, it is possible to identify different kinds of FeCO neurons. Additionally, next section will present the survival analysis and transfer entropy theories. They are followed by the methodology section that describes the experiment. Also, the results section will present the FeCO analysis, followed by the conclusion and next steps.

2 THEORY

This section presents the theories used to analyze the FeCO data, and assemble the models created, respectively Transfer Entropy, and Survival Analysis.

2.1 Transfer Entropy

We used the property of transfer entropy detect time delays (Pampu et al., 2013) as a reference measure to check the algorithms consistency by calculating the propagation time between the signals 200Hz and 27Hz. We also used it to look for dependencies between FeCO and 27Hz signals. Additionally, it will be used to reinforce our assumption of different kinds of FeCO.

Transfer entropy has significant properties. The first one is that it indicates the shared information between two random variables, making possible to determine connections and dependencies (Runge et al., 2012). A second one is that transfer entropy uses a time lag to introduce directional sense (Schreiber, 2000), causal sense (Wibral et al., 2012) and find time-delays (Ito et al., 2011). These properties make it similar to time-delayed mutual information (Jin et al., 2010). However, time-delayed mutual information does not distinguish information exchanged from shared information, while transfer entropy does (Schreiber, 2000).

Transfer entropy (Vicente et al., 2011) is defined as follows by

$$TE(X;Y) = \sum p(y_{t+u}, y_t^{d_y}, x_t^{d_x}) \log \frac{p(y_{t+u}|y_t^{d_y}, x_t^{d_x})}{p(y_{t+u}|y_t^{d_y})}, \quad (1)$$

where t represents the discrete time index, u the prediction time, and $x_t^{d_x}$ and $y_t^{d_y}$ are the delay vectors.

2.2 Survival Analysis

A survival time variable (T) is a non-negative random variable representing the time until an event occurs (Klein and Moeschberger, 2003). If f(t) represents T probability density function, and $F(t)$ represents its cumulative distribution function, then the survival function ($S(t)$) is defined as follows:

$$S(t) = Pr(T \geq t) = 1 - F(t) = \int_t^{\infty} f(x)dx, \quad (2)$$

which represents the probability of an event do not occur during time t.

Another concept related to the survival variable T is the hazard function $h(t)$ defined as:

$$h(t) = \lim_{\Delta t \to 0} \frac{P(t \leq T < t + \Delta t | T \geq t)}{\Delta t}. \quad (3)$$

The function $h(t)$ represents the instantaneous rate of a given event occurs at time t (Klein and Moeschberger, 2003). For $\Delta t \to 0$,

$$P(t \leq T < t + \Delta t) \to f(t) \quad (4)$$

and using the conditional probability rule (Walpole et al., 2014) we can rewrite (3),

$$P(A|B) = \frac{P(A \cap B)}{P(B)} \Rightarrow h(t) = \frac{f(t)}{S(t)}. \quad (5)$$

In the experiments, the excitation signals had a constant bandwidth, hence we considered that the spike rate is also constant. Consequently, the hazard function is also constant, and in this case, it is possible to use an exponential distribution,

$$f(t) = \lambda e^{-\lambda t} = \mu e^{-\frac{t}{\mu}}, \quad (6)$$

with survival function

$$S(t) = e^{-\lambda t} = e^{-\frac{t}{\mu}}, \quad (7)$$

where λ is the spike rate (spikes/ms), and μ is the distribution mean (ms/spike) (Harrell, 2013).

To obtain the exponential models for the data sets, we sampled the time between spikes (ISI), and calculated a mean time between spikes (MTBS - μ) on each one of the signals.

3 MATERIALS AND METHODS

The experiments used thirty five adult desert locusts, *Schistocerca gregaria* (Forskål), male and female, arranged ventral-side-uppermost in modeling clay. By cutting a piece of cuticle in their anterior distal femur, the FeCO apodeme was exposed and gripped by a forceps attached to a shaker (Ling Altec 101). A small window opened in their ventral thorax exposed the metathoracic ganglion that was immobilized on a wax covered with a silver platform. The sheath was treated with protease (Sigma type XIV) for 1 min before recording. After that, microelectrodes filled with potassium acetate and with DC resistances of 50-80 MΩ were driven through the sheath. They entered into the neuropilar processes of the nonspiking local interneurons, the axons of sensory neurons, or the somata of spiking local interneurons. Intracellular recordings were made using an Axoclamp 2A amplifier (Axon Instruments, USA).

A GWN signal shook the forceps. The GWN was produced by filtering a pseudo random binary sequence (CG-742, NF Circuit Design Block) band-limited to 27Hz or 58Hz with low-pass filters (SR-4BL, NF Circuit Design Block) with a decay of 24 dB/octave. This generated a signal with a Gaussian probability density function in the bandwidth of interest. The signal vibrated the forceps holding the apodeme, stimulating and evoking the interneurons responses, as shown in Figure 2. The signals were stored on magnetic tape using a PCM-DAT data recorder (RD-101 T, TEAC, Japan) and then sampled at a rate of 10 kHz offline to a computer.

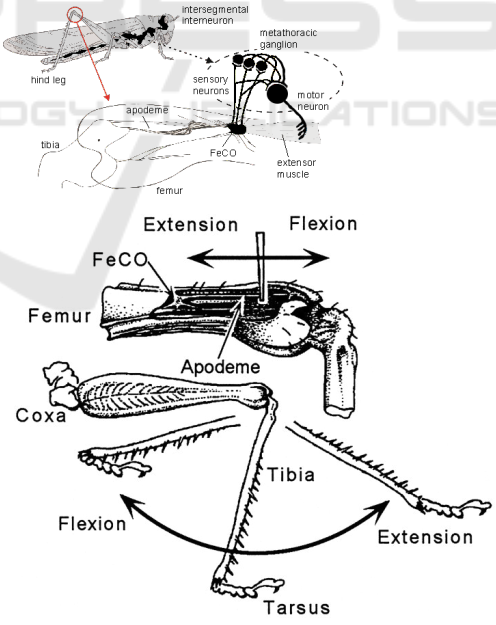

Figure 2: Desert Locust neuronal system (top) with the neurons where the signals were collected, highlighting the FeCO. Correspondent leg movement for the extension/flexing caused by the forceps excitation (bottom).

4 RESULTS

This section presents the ISI Analysis on 27Hz, and 58Hz signals, and transfer entropy measurements in the 27Hz signals.

4.1 ISI Analysis

Experiment with 27Hz Signals

The MTBS on each one of the 27Hz signals were measured, and their confidence intervals were calculated. Table 1 shows the results after processing the 27Hz data set, calculating the MTBS and confidence intervals considering an $\alpha = 5\%$ for all 25 samples.

Table 1: MTBS and confidence intervals for 27Hz signals.

Sample	CI Low (ms/spike)	MTBS (ms/spike)	CI Up (ms/spike)
1	15.79	16.92	18.05
2	19.52	20.32	21.12
3	21.69	22.50	23.30
4	21.75	22.60	23.45
5	21.72	22.67	23.61
6	22.01	23.01	24.02
7	21.95	23.18	24.40
8	22.46	23.49	24.52
9	23.73	24.66	25.58
10	24.06	25.35	26.65
11	24.45	25.56	26.68
12	25.68	26.91	28.15
13	26.14	28.71	31.27
14	28.42	29.89	31.35
15	30.75	32.63	34.50
16	31.42	33.05	34.69
17	33.25	35.84	38.43
18	34.95	36.82	38.69
19	45.31	49.10	52.89
20	46.83	49.79	52.76
21	46.85	49.83	52.80
22	50.00	53.26	56.53
23	51.90	54.12	56.34
24	58.15	62.16	66.18
25	58.14	62.28	66.41

Table 1, presents a gap between samples 18 and 19 confidence intervals. The same gap appears in the MTBS histogram presented in Figure 3. These gaps point to the existence of two groups, i.e., two different neuronal responses rates.

Since samples 1 and 2 confidence intervals are disconnected, we performed a hypothesis test comparing the MTBS, testing if there are two or three groups of neurons (Walpole et al., 2014). The tests assumed a t statistic with an $\alpha = 5\%$, and followed the hypothesis

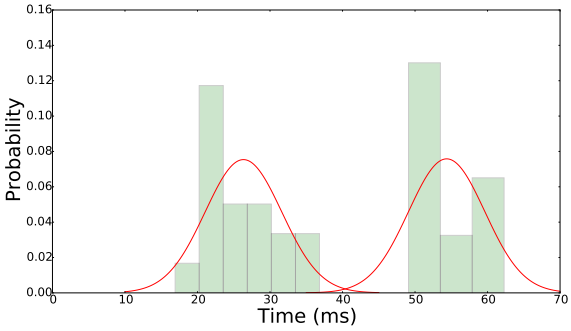

Figure 3: Histogram of the MTBS (Table 1) calculated for the 25 signals in the 27Hz data set. It is possible to note a gap indicating the presence of two different groups.

$$\begin{cases} H_0 : \mu = \mu_i \\ H_1 : \mu \neq \mu_i. \end{cases} \quad (8)$$

The hypothesis H_0 indicates that the MTBS measured (μ_i) is equal to the group mean (μ), while the hypothesis H_1 indicates the opposite. The hypothesis H_0 was accepted with a significance level $\alpha = 5\%$ for all MTBS inside each group.

Experiment with 58Hz Signals

The time between each spike on the 58Hz signals was measured in order to calculate the MTBS and their confidence intervals. Table 2 shows the results after processing all the 58Hz data set, calculating the MTBS and confidence intervals considering an $\alpha = 5\%$.

From Table 2, it is possible to see that the samples confidence intervals cannot be separated. This suggests only one group of neurons in the 58Hz data. This is reinforced by Figure 4 that shows the histogram of MTBS. To assure this assumption, a hypothesis test (Equation 8) for the MTBS was made with an $\alpha = 5\%$. As a result, the hypothesis H_0 was accepted for all MTBS (μ_i).

A consideration must be made for the 58Hz experiment, since its results opposed to the ones presented in Figure 3. The number of samples in the 58Hz experiment is the same of the first group found in the 27Hz experiment; thence it is possible that the 58Hz experiment only recorded signals from the first group. However, it is known that there are nonlinear components in the desert locust neuronal system (Dewhirst et al., 2013). This implies that the output signal could present an entirely different response once that the input excitation is changed.

Table 2: MTBS and confidence intervals for 58Hz signals.

Sample	CI Low (ms/spike)	MTBS (ms/spike)	CI Up (ms/spike)
1	17.87	18.57	19.27
2	18.33	19.03	19.73
3	19.23	19.92	20.60
4	19.38	20.12	20.87
5	19.40	20.15	20.90
6	19.53	20.35	21.18
7	19.58	20.37	21.16
8	19.67	20.43	21.19
9	19.88	20.69	21.50
10	20.51	21.32	22.13
11	21.82	22.84	23.86
12	22.43	23.46	24.48
13	22.56	23.46	24.36
14	22.96	24.12	25.28
15	24.84	25.79	26.74
16	25.45	26.53	27.60
17	27.36	29.17	30.98
18	28.86	30.17	31.47

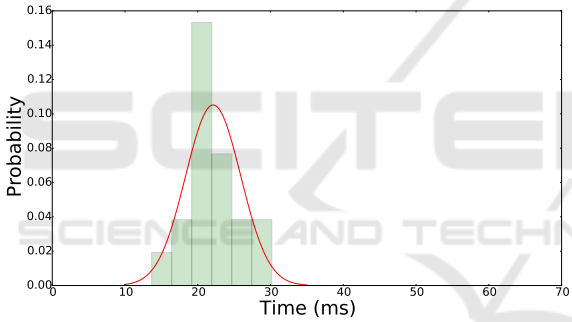

Figure 4: Histogram of MTBS (Table 2) calculated for the 18 signals in the 58Hz data set. It is possible to note only one group of neurons.

4.2 Transfer Entropy

After making ISI analyzes and find evidences of two possible kinds of neuronal response in the 27Hz data set, we made transfer entropy measurements for the signals inside the 27Hz experiment.

The filter used adds a fixed and well known time delay for a given cutoff frequency f_c (Manal and Rose, 2007). The equation for the time delay is given by

$$t_{delay} = \frac{0.416}{f_c}, \tag{9}$$

and since f_c was 27Hz, it is expected that transfer entropy presents a 15.41ms delay between 200Hz and 27Hz signals. Figure 5 shows that the time-delay found is close to the expected.

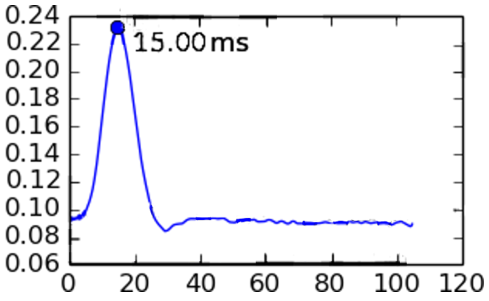

Figure 5: Transfer entropy calculated between 200Hz and 27Hz signals for references purposes. The time delay found is close to the expected with an error of 2.6%.

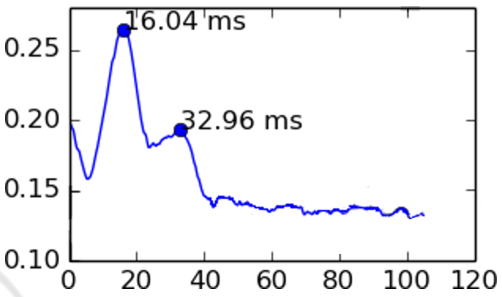

Figure 6: Transfer entropy calculated between 27Hz and FeCO signals in the first group of neurons, showing two maximum points.

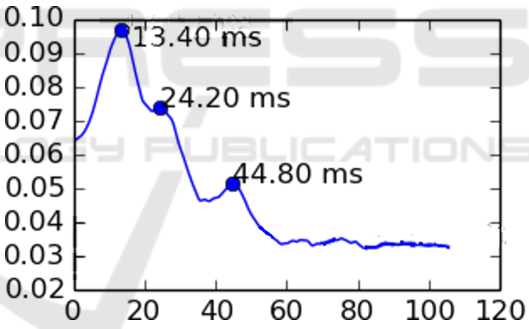

Figure 7: Transfer entropy calculated between 27Hz and FeCO signals in the second group of neurons, showing three maximum points.

We calculated transfer entropy between 27Hz and FeCO signals in the first group, which is presented in Figure 6. It is important to note that the graph shows two maximum points.

We also calculated transfer entropy between 27Hz and FeCO signals in the second group. Figure 7 presents the results and points three time-delays.

Figure 6 differs from Figure 7 in the number of time-delays found. The first figure presents two maximum points: one at 16.04 ms, and another at 32.96 ms. The second presents three maximums: one at 13.40 ms, other at 24.20 ms, and another at 44.80 ms.

4.3 FeCO Survival Models

We found two groups of neurons in the 27Hz experiment and one group in the 58Hz. Using MTBS it is possible to construct models representing their response due to a fixed excitation. Thence, it is considered the Survival models for that construction.

Considering that the distribution mean is the mean of the group, we calculated confidence intervals with an $\alpha = 5\%$ for each group mean, as shown in Table 3.

Table 3: Parameters calculated for the 27Hz experiment.

Group	λ (spikes/ms)	μ (ms/spike)	CI 95% Low	CI 95% Up
1st	0.04	26.34	23.64	29.04
2nd	0.02	54.36	51.55	57.12

Figure 8 presents a graphic visualization, and it is possible to notice that there is no common region either for the functions or their confidence intervals.

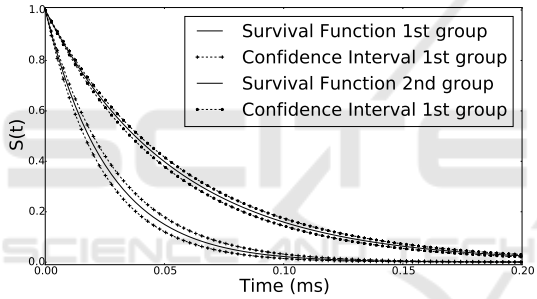

Figure 8: Survival probability functions for the two groups of neurons. The confidence intervals of those groups do not touch, evidencing the existence of two groups of neurons.

In the 58Hz experiment we found only one neuronal response rate. Considering that the distribution mean is the group mean, we calculated a confidence interval with an $\alpha = 5\%$ for the group, as shown in Table 4.

Table 4: Parameters calculated for the 58Hz experiment.

Group	λ (spikes/ms)	μ (ms/spike)	CI 95% Low	CI 95% Up
1st	0.05	22.11	20.89	24.27

4.4 FeCO Model

Results pointed two different neuronal responses, which brings two possibilities. The first one is that it happens because there are two different FeCO structures. The second is that it happens because of the neuronal configuration. Figure 10 presents three hypothetical neuronal configurations.

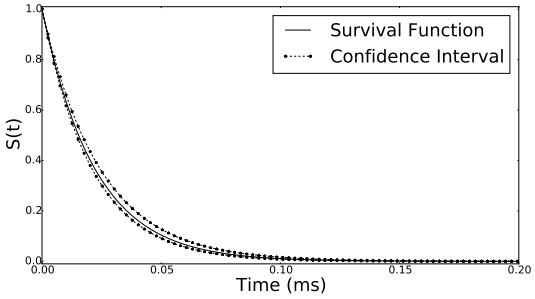

Figure 9: Survival probability function for the group of neurons found in the 58Hz data set with its confidence intervals.

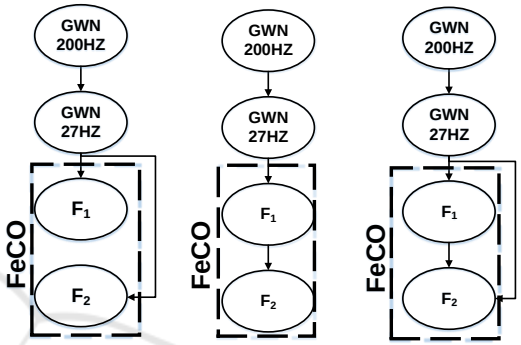

Figure 10: Models suggested for the FeCO. A model with two different neurons that are independent (left). Other model where only the fist kind of FeCO affects the second type (middle). A model showing an influence of the first kind of FeCO, but it also presenting a direct influence of the 27Hz signal on the second kind of FeCO (right).

The structures from Figure 10 are only suggestions for the neuronal circuit configuration, which need deeper investigations to confirm. The first configuration assumes two different kinds of FeCO, and they receive direct influence from the excitation signal. The second and the third configurations can assume two distinct kinds of FeCO or only just two different response rates given by the same kind of FeCO with different configurations. Both, third and second configurations, suggest a model organized in layers where there is a preprocessing process.

5 CONCLUSION

In this paper, we used two analyzes to investigate different neuronal responses due to the same excitation. We analyzed signals from the desert locust metathoracic ganglion. Specifically we looked at the data from the Desert Locust Femorotibial Chordotonal Organ, which is a spiking neuron. The diagram shown in Figure 1 was the simplest representation possible for

the FeCo experiment, ignoring the existence of any other kind of FeCO neurons.

Figure 1 presented a diagram connecting the 200Hz signals to the 27Hz signals, and then 27Hz to FeCO, and does not consider any other influences, such as other neurons. However, here we pointed evidence that suggest the existence of different kinds of FeCO neurons. These findings show that it is possible to obtain different response rates for FeCO neurons even when they receive the same stimulation. Therefore, it implies that there is a different connection than the one presented in Figure 1.

Our assumption of a different connection than the one showed in Figure 1 is supported by three different analyses. The histograms of MTBS from Figure 3 pointed the existence of different neurons using the ISI technique, and statistical hypothesis tests supports these results. The survival models also showed two different curves with non-overlapping confidence intervals. Additionally, Figure 6 and Figure 7 shows two different responses for each group using the transfer entropy technique.

All these measurements and tests point the existence of more than one kind of FeCO neuron. A consideration must be made for the 58Hz signals since they presented only one group, a result different than the one showed for 27Hz signals. It is known that there are nonlinear components inside the neuronal system (Dewhirst et al., 2013), and this implies that the output response could be entirely different once the input excitation is changed.

We know that the algorithms for transfer entropy are correct because of the reference measurement presented in Figure 5. A closer look at Figure 7 indicates that it presents one more maximum point than Figure 6. By comparing the responses of Figure 6 and Figure 7 we made new assumptions about the connections inside the FeCO, they are presented in Figure 10.

The assumptions presented in Figure 10 suggest two particular cases. The first one with a structure where there are no influence or iterations between the two kinds of FeCO. The second case is that there is an interaction between them. This case is supported by Figure 7 that presents one more maximum point than Figure 6, indicating a model organized in layers.

Those three possible structures shown in Figure 10 are not the only possible configuration for the neuronal system; the locust may have a complex structure. Future works are required to determine the best connections and the best structure. Therefore, this is our next steps when we intend to investigate the best structure model using Dynamical Bayesian Networks (Meyer-Baese and Schmid, 2014).

Moreover, this analysis indicates that the FeCO neuronal connection structure is more complex than the one presented in Figure 1. Additionally, we presented models based on survival functions for the FeCO response. Those models can also be used to perform simulations in future works.

ACKNOWLEDGEMENT

The authors would like to thank the Brazilian Federal Agency for Support and Evaluation of Graduate Education - CAPES; and also thank the National Counsel of Technological and Scientific Development CNPq for the Project number 475064/2013-5.

REFERENCES

Achcar, J. A. and Moala, F. A. (2015). Use of copula functions for the reliability of series systems. *International Journal of Quality & Reliability Management*, 32(6):617–634.

Angarita-Jaimes, N., Dewhirst, O. P., Simpson, D. M., Kondoh, Y., Allen, R., and Newland, P. L. (2012). The dynamics of analogue signalling in local networks controlling limb movement. *European Journal of Neuroscience*, 36(9):3269–3282.

Barnett, L., Barrett, A. B., and Seth, A. K. (2009). Granger causality and transfer entropy are equivalent for gaussian variables. *Phys. Rev. Lett.*, 103:238701.

Bewick, V., Cheek, L., and Ball, J. (2004). Statistics review 12: survival analysis. *CRITICAL CARE-LONDON-*, 8:389–394.

Birmingham, K., Gradinaru, V., Anikeeva, P., Grill, W. M., Pikov, V., McLaughlin, B., Pasricha, P., Weber, D., Ludwig, K., and Famm, K. (2014). Bioelectronic medicines: a research roadmap. *Nature Reviews Drug Discovery*, 13(6):399–400.

Burrows, M., Laurent, G., and Field, L. (1988). Proprioceptive inputs to nonspiking local interneurons contribute to local reflexes of a locust hindleg. *The Journal of neuroscience*, 8(8):3085–3093.

Cabrero, M., Jabbour, E., Ravandi, F., Bohannan, Z., Pierce, S., Kantarjian, H. M., and Garcia-Manero, G. (2015). Discontinuation of hypomethylating agent therapy in patients with myelodysplastic syndromes or acute myelogenous leukemia in complete remission or partial response: Retrospective analysis of survival after long-term follow-up. *Leukemia Research*, 39(5):520 – 524.

Chen, L., Deng, Y., Luo, W., Wang, Z., and Zeng, S. (2009). Detection of bursts in neuronal spike trains by the mean inter-spike interval method. *Progress in Natural Science*, 19(2):229 – 235.

Collett, D. (2003). *Modelling survival data in medical research*. Texts in statistical science. Chapman & Hall, London, New York.

Dewhirst, O., Angarita-Jaimes, N., Simpson, D., Allen, R., and Newland, P. (2013). A system identification analysis of neural adaptation dynamics and nonlinear responses in the local reflex control of locust hind limbs. *Journal of Computational Neuroscience*, 34(1):39–58.

Endo, W., Santos, F., Simpson, D., Maciel, C., and Newland, P. (2015). Delayed mutual information infers patterns of synaptic connectivity in a proprioceptive neural network. *Journal of Computational Neuroscience*, 38(2):427–438.

Harrell, F. E. (2013). *Regression modeling strategies: with applications to linear models, logistic regression, and survival analysis*. Springer Science & Business Media.

Ito, S., Hansen, M. E., Heiland, R., Lumsdaine, A., Litke, A. M., and Beggs, J. M. (2011). Extending transfer entropy improves identification of effective connectivity in a spiking cortical network model. *PLoS ONE*, 6(11):e27431.

Jegadeesan, R., Thakor, N., and Yen, S. C. (2015). Wireless for peripheral nerve prosthesis and safety. In *Neural Engineering (NER), 2015 7th International IEEE/EMBS Conference on*, pages 648–651.

Jimnez-Fabin, R. and Verlinden, O. (2012). Review of control algorithms for robotic ankle systems in lower-limb orthoses, prostheses, and exoskeletons. *Medical Engineering & Physics*, 34(4):397 – 408.

Jin, S.-H., Lin, P., and Hallett, M. (2010). Linear and nonlinear information flow based on time-delayed mutual information method and its application to corticomuscular interaction. *Clinical Neurophysiology*, 121(3):392–401.

Klein, J. P. and Moeschberger, M. L. (2003). *Survival analysis: techniques for censored and truncated data*. Springer Science & Business Media.

Lawless, J. F. (2011). *Statistical models and methods for lifetime data*, volume 362. John Wiley & Sons.

Maciel, C. D., Simpson, D. M., and Newland, P. L. (2012). Inference about multiple pathways in motor control limb in locust. In *BIOSIGNALS*, pages 69–75.

MacKenzie, T., Gifford, A. H., Sabadosa, K. A., Quinton, H. B., Knapp, E. A., Goss, C. H., and Marshall, B. C. (2014). Longevity of patients with cystic fibrosis in 2000 to 2010 and beyond: survival analysis of the cystic fibrosis foundation patient registry. *Annals of internal medicine*, 161(4):233–241.

Manal, K. and Rose, W. (2007). A general solution for the time delay introduced by a low-pass butterworth digital filter: An application to musculoskeletal modeling. *Journal of Biomechanics*, 40(3):678 – 681.

Meyer-Baese, A. and Schmid, V. J. (2014). *Pattern Recognition and Signal Analysis in Medical Imaging*. Elsevier.

Newland, P. L. and Kondoh, Y. (1997). Dynamics of neurons controlling movements of a locust hind leg ii. flexor tibiae motor neurons. *Journal of Neurophysiology*, 77(4):1731–1746.

Nichols, J., Seaver, M., Trickey, S., Todd, M., Olson, C., and Overbey, L. (2005). Detecting nonlinearity in structural systems using the transfer entropy. *Physical Review E*, 72(4):046217.

Pampu, N., Vicente, R., Muresan, R., Priesemann, V., Siebenhuhner, F., and Wibral, M. (2013). Transfer entropy as a tool for reconstructing interaction delays in neural signals. In *Signals, Circuits and Systems (ISSCS), 2013 International Symposium on*, pages 1–4.

Runge, J., Heitzig, J., Marwan, N., and Kurths, J. (2012). Quantifying causal coupling strength: A lag-specific measure for multivariate time series related to transfer entropy. *Phys. Rev. E*, 86:061121.

Santos, F. P. and Maciel, C. D. (2014). A pso approach for learning transition structures of higher-order dynamic bayesian networks. In *Biosignals and Biorobotics Conference (2014): Biosignals and Robotics for Better and Safer Living (BRC), 5th ISSNIP-IEEE*, pages 1–6.

Schreiber, T. (2000). Measuring information transfer. *Physical review letters*, 85(2):461.

Schwalger, T., Droste, F., and Lindner, B. (2015). Statistical structure of neural spiking under non-poissonian or other non-white stimulation. *Journal of Computational Neuroscience*, 39(1):29–51.

Subramaniam, K., Hooker, C. I., Biagianti, B., Fisher, M., Nagarajan, S., and Vinogradov, S. (2015). Neural signal during immediate reward anticipation in schizophrenia: Relationship to real-world motivation and function. *NeuroImage: Clinical*, 9:153 – 163.

Vicente, R., Wibral, M., Lindner, M., and Pipa, G. (2011). Transfer entropya model-free measure of effective connectivity for the neurosciences. *Journal of Computational Neuroscience*, 30(1):45–67.

Vidal-Gadea, A. G., Jing, X., Simpson, D., Dewhirst, O. P., Kondoh, Y., Allen, R., and Newland, P. L. (2010). Coding characteristics of spiking local interneurons during imposed limb movements in the locust. *Journal of neurophysiology*, 103(2):603–615.

Walpole, R., Myers, R., Myers, S., and Ye, K. (2014). Probability and statistics for engineers and scientists.

Wibral, M., Wollstadt, P., Meyer, U., Pampu, N., Priesemann, V., and Vicente, R. (2012). Revisiting wiener's principle of causality #x2014; interaction-delay reconstruction using transfer entropy and multivariate analysis on delay-weighted graphs. In *Engineering in Medicine and Biology Society (EMBC), 2012 Annual International Conference of the IEEE*, pages 3676–3679.

Zhang, Q., Yang, X., Li, P., Huang, G., Feng, S., Shen, C., Han, B., Zhang, X., Jin, F., Xu, F., and Lu, T. J. (2015). Bioinspired engineering of honeycomb structure using nature to inspire human innovation. *Progress in Materials Science*, 74:332 – 400.